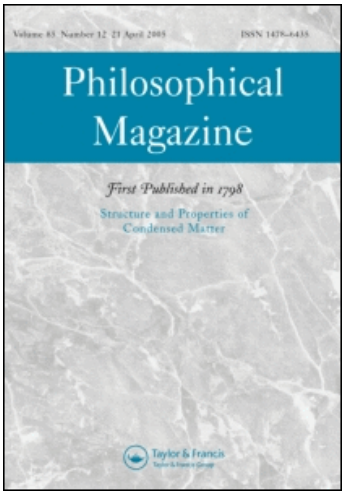

Philosophical Magazine
Publication details, including instructions for authors and subscription information:
http://www.informaworld.com/smpp/title~content=t713695589

Graphene under perpendicular incidence of electromagnetic waves: Gaps and band structure

F. J. López-Rodríguez[a]; G. G. Naumis[a]
[a] Departamento de Física-Química, Instituto de Física, Universidad Nacional Autónoma de México (UNAM), México D.F., México

Online publication date: 02 June 2010

To cite this Article López-Rodríguez, F. J. and Naumis, G. G.(2010) 'Graphene under perpendicular incidence of electromagnetic waves: Gaps and band structure', Philosophical Magazine, 90: 21, 2977 — 2988
To link to this Article: DOI: 10.1080/14786431003757794
URL: http://dx.doi.org/10.1080/14786431003757794

Philosophical Magazine
Vol. 90, No. 21, 21 July 2010, 2977–2988

Taylor & Francis
Taylor & Francis Group

Graphene under perpendicular incidence of electromagnetic waves: Gaps and band structure

F.J. López-Rodríguez and G.G. Naumis*

Departamento de Física-Química, Instituto de Física, Universidad Nacional Autónoma de México (UNAM), Apartado Postal 20-364, 01000, México D.F., México

(*Received 7 December 2009; final version received 7 March 2010*)

We study the energy spectrum for the problem of graphene's carriers under perpendicular incidence of electromagnetic waves. To obtain the spectrum, we solve the Dirac equation under such a field. Then a generalized Mathieu equation is obtained. The limiting cases of strong and weak fields, as well as long and short wavelengths, are analyzed. The energy spectrum is obtained numerically by using the Whittaker method, and a perturbation method is used to obtain the analytical separatrix curve between allowed and forbidden states. The energy spectrum presents bands, and a gap at the Fermi energy. The gap is linear on the electromagnetic wave intensity.

Keywords: graphene; electromagnetic waves; Mathieu equation; gaps

1. Introduction

In the last four and a half years, graphene (a two-dimensional allotrope of carbon) has become the corner-stone of much research [1–3]. Since its discovery in 2004, using the technique called micromechanical cleavage [4], different groups have studied experimentally its properties and potential applications. Graphene, for example, has a breaking strength 200 times greater than steel [5]. With this material, scientists have achieved electron mobilities of 200,000 $cm^2\ V^{-1}\ s^{-1}$ by suspending single layer graphene [6]. However, when graphene is set in a substrate, mobilities decrease [7]. The mobilities are now $\sim 4 \times 10^4\,cm^2\ V^{-1}\ s^{-1}$ indicating the importance of the choice of substrate. On the other hand, because of these high mobilities, there has been much effort to use graphene in electronic devices. One of the first technological achievements was to make the first single electron transistor [8], and the operation of the first graphene transistor at GHz frequencies [9].

On the theoretical side, much effort has been devoted to understanding the electromagnetic properties of graphene [10–21]. Among this work we can mention the studies of the frequency dependant conductivity [10,11,17,18], the nonlinear electromagnetic response of graphene [19,20], the novel electric field effects [13] and

*Corresponding author. Email: naumis@fisica.unam.mx

ISSN 1478–6435 print/ISSN 1478–6443 online

DOI: 10.1080/14786431003757794
http://www.informaworld.com

the possibility to induce a gap by applying magnetic and electric fields [20,21]. This effect can also be induced by doping graphene [22], and its prediction has been confirmed very recently [23].

In previous work, we studied the problem of graphene irradiated by electromagnetic waves [20]. We showed that graphene takes an incoming electrical signal of determinate frequency and produces an output signal whose frequency is a multiple of the original one. Therefore graphene can work as a frequency multiplier. Recently the materialization of this idea was achieved at the Massachusetts Institute of Technology where David Chandler and collaborators built the first experimental graphene frequency multiplier [24]. However, in our previous derivation, the solution contained a very rough approximation, since the second derivative of the field was neglected [20]. Here we provide a solution that avoids this problem, and solves the inconsistencies of the previous solution. Furthermore, in our previous work we only considered the case of electromagnetic radiation with a wavevector in the graphene plane. In most of the experimental situations, the radiation has normal incidence to the graphene. For example, this is the case for most of the optical properties. In this paper, we continue the research into graphene interacting with radiation, but now we consider the important case of a graphene layer irradiated with perpendicular incidence of an electromagnetic plane wave. By solving a new kind of generalized Mathieu equation, we obtain the spectrum of energies, which presents bands and gaps. In the limit of high frequencies or small fields, the gap is at the Fermi energy and thus can influence the transport properties.

The paper is organized as follows. In Section 2, we show how to model the interaction between the electric field and the sample of graphene. We find three important limiting cases to analyze, corresponding to interesting experimental situations. In Section 3 we study in detail all the limiting cases; in Section 4 the conclusion are given; and the details of the calculations are summarized in the appendixes.

2. Modelling graphene under a perpendicular electromagnetic field

For graphene, it has been shown that the Hamiltonian for wavevectors close to the K point of the first Brioullin zone can be written as [25],

$$H(x,y,t) = v_F \begin{pmatrix} \epsilon_0 & \hat{\pi}_x - i\hat{\pi}_y \\ \hat{\pi}_x + i\hat{\pi}_y & \epsilon_0 \end{pmatrix}, \tag{1}$$

where v_F is the Fermi velocity $v_F \approx c/300$, with c the light speed. ϵ_0 is the zero point energy, $\hat{\pi} = \hat{\mathbf{p}} - e\mathbf{A}/c$ with $\hat{\mathbf{p}}$ being the electron momentum operator, and $\mathbf{A}$ is the vector potential of the applied electromagnetic field, given by $\mathbf{A} = (\frac{E_0}{\omega}\cos(kz - \omega t), 0)$. E_0 is the amplitude of the electric field and ω is the frequency of the wave. E_0 can be taken as a constant since screening effects are weak in graphene [26]. The dynamics of charge carriers in graphene is governed by the Dirac equation [25],

$$H(x,y,t)\mathbf{\Psi}(x,y,t) = i\hbar \frac{\partial \mathbf{\Psi}(x,y,t)}{\partial t}, \tag{2}$$

where,

$$\mathbf{\Psi}(x,y,t) = e^{-i\epsilon_0 t/\hbar}\begin{pmatrix}\Psi_A(x,y,t)\\ \Psi_B(x,y,t)\end{pmatrix}, \tag{3}$$

is a two component spinor. Here A and B stand for each sublattice index of the bipartite graphene lattice [27]. Inserting Equation (3) into Equation (2) we obtain,

$$v_F(\hat{\pi}_x - i\hat{\pi}_y)\Psi_B(x,y,t) = i\hbar\frac{\partial\Psi_A(x,y,t)}{\partial t}, \tag{4}$$

$$v_F(\hat{\pi}_x + i\hat{\pi}_y)\Psi_A(x,y,t) = i\hbar\frac{\partial\Psi_B(x,y,t)}{\partial t}. \tag{5}$$

The commutation rules for $\hat{\pi}_x$, $\hat{\pi}_y$ and $\partial/\partial t$ are in this case,

$$\left[\hat{\pi}_i, \hat{\pi}_j\right] = 0, \quad i,j = x,y \tag{6}$$

$$\left[\frac{\partial}{\partial t}, \hat{\pi}_x \pm i\hat{\pi}_y\right] = -\frac{eE_o}{c}\sin(kz - \omega t). \tag{7}$$

Using these commutation rules and Equations (4) and (5), we find the following equation of motion for the spinor under the electromagnetic field,

$$-\hbar^2\left(v_F^2\left(\frac{\partial^2\mathbf{\Psi}}{\partial x^2} + \frac{\partial^2\mathbf{\Psi}}{\partial y^2}\right) - \frac{\partial^2\mathbf{\Psi}}{\partial t^2}\right) + 2i\hbar\xi v_F\cos\phi\frac{\partial\mathbf{\Psi}}{\partial x} + \left[\xi^2\cos^2\phi - i\hbar\omega\xi\sigma_x\sin\phi\right]\mathbf{\Psi} = 0, \tag{8}$$

where we have defined the phase ϕ of the electromagnetic wave as $\phi = kz - \omega t$. The parameter ξ is defined as,

$$\xi = \frac{eE_0 v_F}{c\omega}, \tag{9}$$

and σ_μ is the set of Pauli matrices. For nearly flat graphene, we can put $z = 0$, and the last equation becomes,

$$\begin{aligned}-\hbar^2\left(v_F^2\left(\frac{\partial^2\mathbf{\Psi}}{\partial x^2} + \frac{\partial^2\mathbf{\Psi}}{\partial y^2}\right) - \frac{\partial^2\mathbf{\Psi}}{\partial t^2}\right) + 2i\hbar\xi v_F\cos(\omega t)\frac{\partial\mathbf{\Psi}}{\partial x}\\ + \left[\xi^2\cos^2(\omega t) - i\hbar\omega\xi\sigma_x\sin(\omega t)\right]\mathbf{\Psi} = 0.\end{aligned} \tag{10}$$

Consider a solution of the following form,

$$\mathbf{\Psi}(x,y,t) = e^{ip_x x/\hbar + ip_y y/\hbar}\mathbf{F}(\omega t), \tag{11}$$

where $\mathbf{F}(\omega t)$ is a spinor. By inserting Equation (11) into Equation (10), it yields an equation for $\mathbf{F}$ (ωt). The resulting differential equation is,

$$\mathbf{F}''(\omega t) + \left\{\frac{\epsilon^2}{(\hbar\omega)^2} + \frac{1}{(\hbar\omega)^2}\left[\xi^2\cos^2(\omega t) - 2\xi v_F p_x\cos(\omega t)\right] - \frac{i\xi}{\hbar\omega}\sigma_x\sin(\omega t)\right\}\mathbf{F}(\omega t) = 0, \tag{12}$$

where $\epsilon = v_F\sqrt{p_x^2 + p_y^2}$. This equation is in fact a set of two coupled differential equations; its solution gives the answer to the problem. The general solution of this equation can be performed by using a method similar to the one presented in Appendix 1. However, the solution is very difficult and here we prefer to present three important limiting cases. One is $\xi = 0$, which serves to check the equation. The others concern the experimental situations $\xi/\hbar\omega \gg 1$ and $\xi/\hbar\omega \ll 1$. Since,

$$\frac{\xi}{\hbar\omega} = \frac{v_F}{c}\frac{eE_0}{\hbar\omega^2} \approx \frac{1}{300}\frac{eE_0}{\hbar\omega^2}, \tag{13}$$

the first case $eE_0/\hbar\omega^2 \gg 300$ corresponds to strong electric fields or long wavelengths, while the case $eE_0/\hbar\omega^2 \ll 300$ corresponds to weak electric fields or short wavelengths. We must mention that our approach breaks down for very strong electromagnetic fields or high frequencies, since the original tight-binding Hamiltonian can be modified in a substantial way. The limiting frequency for using the Dirac model is around [28] $\omega \sim 4 \times 10^{15}$ Hz. Having these considerations in mind, let us explore the nature of the solutions in the following section.

3. Approximate solutions

3.1. *No electric field*

The first case is when $\xi = 0$; this means that there is no interaction between charge carries and the electromagnetic wave, thus we have free particles in the graphene sheet. The equation for $\mathbf{F}(\omega t)$ is

$$\mathbf{F}''(\omega t) + \frac{\epsilon^2}{(\hbar\omega)^2}\mathbf{F}(\omega t) = 0 \tag{14}$$

whose solution is

$$\mathbf{F}(\omega t) = e^{\pm i\epsilon t/\hbar}\mathbf{u}. \tag{15}$$

This last equation is the solution of the free particle problem as it should be. Here $\mathbf{u}$ is a spinor that can be written as

$$\mathbf{u} = \frac{1}{\sqrt{2}}\begin{pmatrix} \pm e^{-i\varphi/2} \\ e^{i\varphi/2} \end{pmatrix}, \quad \varphi = \tan\left(\frac{p_y}{p_x}\right),$$

where the plus and minus sign stand for electrons and holes, respectively.

3.2. *Intense electric fields or long wavelengths ($eE_0/\hbar\omega^2 \gg 300$)*

In this case $\xi/\hbar\omega \gg 1$, and thus in Equation (12) we can neglect linear terms in $\xi/\hbar\omega$. Also, in what follows we take $p_x = 0$, which is basically an initial condition, in order to simplify the equations, although the general case can be solved in a similar way. The following equation is obtained for $\mathbf{F}(\omega t)$,

$$\mathbf{F}''(\omega t) + \left\{\frac{\epsilon^2}{(\hbar\omega)^2} + \frac{1}{(\hbar\omega)^2}\xi^2\cos^2(\omega t)\right\}\mathbf{F}(\omega t) = 0. \tag{16}$$

Using the relation $\cos^2(\omega t) = \frac{1}{2}(1 + \cos(2\omega t))$ we can write,

$$\mathbf{F}''(\omega t) + \left\{ \frac{\epsilon^2}{(\hbar\omega)^2} + \frac{\xi^2}{(\hbar\omega)^2}\left[\frac{1}{2}(1 + \cos(2\omega t)\right]\right\} F(\omega t) = 0,$$

and defining,

$$q = -\frac{\xi^2}{4(\hbar\omega)^2}, \tag{17}$$

and,

$$a = \frac{\epsilon^2}{(\hbar\omega)^2} - 2q, \tag{18}$$

we obtain the equation

$$\frac{\mathrm{d}^2\mathbf{F}(\omega t)}{\mathrm{d}\,(\omega t)^2} + (a - 2q\cos(2\omega t))\mathbf{F}(\omega t) = 0, \tag{19}$$

which is a set of two uncoupled Mathieu equations in standard form. According to Floquet's theory, the solution of Equation (19) has the form [29],

$$F(\omega t) = \sum_{r=-\infty}^{\infty} C_{2r}(\mu; a, q) e^{(\mu + 2ri)\omega t}, \tag{20}$$

where $C_{2r}(\mu; a, q)$ are Fourier coefficients. Furthermore, using the Whittaker method, in Appendix 1 we show that the allowed values of μ are given by,

$$\mu = \frac{1}{\pi}\cos^{-1}(1 - \Delta_r(0; a, q)(1 - \cos\pi\sqrt{a})) \quad a \geq 0, \tag{21}$$

and

$$\mu = \frac{1}{\pi}\cos^{-1}(1 - \Delta_r(0; a, q)(1 - \cosh\pi\sqrt{a})) \quad a < 0. \tag{22}$$

where $\Delta_r(0; a, q)$ is a determinant defined in Appendix 1, which can be calculated using the recursive Strang method [29].

In Figure 1 we present the energy spectrum obtained from Equations (21) and (22), in which the gray regions are the allowed values of the energy. This diagram is the spectrum of the usual Mathieu equation. However, in the present case there is an extra constraint that relates a with q due to Equation (18). For fixed energies ϵ, this condition is equivalent to drawing a set of parallel lines in Figure 1. Since $(\epsilon/\hbar\omega)^2$ is always positive, in Figure 1 we plot the line $a = -2q$, which divides the spectrum into two zones. Energies on the left side of this line are not allowed, while the values on the right side are allowed. States over this line have $\epsilon = 0$. Notice that for a fixed electric field, q is a constant. Thus, to 'read' the spectrum for a given field, one must draw a vertical line at fixed q. Using this method, a simple analysis of Figure 1 reveals bands separated by energy gaps.

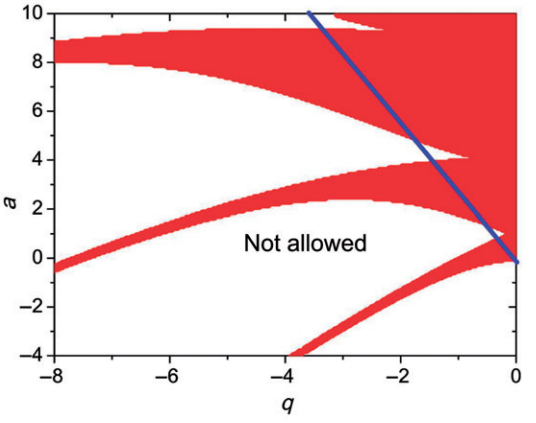

Figure 1. Energy spectrum for the case of intense electric fields or long wavelengths. A line divides the spectrum into two regions; one of them is allowed while the other is forbidden due to Equation (18).

3.3. *Weak electric field or short wavelengths ($eE_0/\hbar\omega^2 \ll 300$)*

Under this limit, in Equation (12) we can neglect quadratic terms in $\xi/\hbar\omega$ to obtain the following equation for $\mathbf{F}(\omega t)$,

$$\mathbf{F}''(\omega t) + \left\{\frac{\epsilon^2}{(\hbar\omega)^2} - \frac{1}{\hbar\omega} i\xi\sigma_x \sin(\omega t)\right\}\mathbf{F}(\omega t) = 0. \tag{23}$$

Equation (23) is a set of two coupled equations. To decouple these equations, we proceed in the following way. First we write both equations explicitly,

$$F_1''(\omega t) + \frac{\epsilon^2}{(\hbar\omega)^2} F_1(\omega t) - \frac{i\xi}{\hbar\omega}\sin(\omega t) F_2(\omega t) = 0, \tag{24}$$

$$F_2''(\omega t) + \frac{\epsilon^2}{(\hbar\omega)^2} F_2(\omega t) - \frac{i\xi}{\hbar\omega}\sin(\omega t) F_1(\omega t) = 0. \tag{25}$$

If we add both equations, we obtain,

$$u''(\omega t) + \left\{\frac{\epsilon^2}{(\hbar\omega)^2} - \frac{1}{\hbar\omega} i\xi \sin(\omega t)\right\}u(\omega t) = 0, \tag{26}$$

where $u\,(\omega t) = F_1(\omega t) + F_2(\omega t)$, while if we subtract them, the following equation is obtained,

$$v''(\omega t) + \left\{\frac{\epsilon^2}{(\hbar\omega)^2} + \frac{1}{\hbar\omega} i\xi \sin(\omega t)\right\}v(\omega t) = 0, \tag{27}$$

where $v\,(\omega t) = F_1(\omega t) - F_2(\omega t)$. For this case, we define new values for a and q,

$$a = \frac{\epsilon^2}{(\hbar\omega)^2}, \tag{28}$$

and,

$$q = \frac{\xi}{2\hbar\omega}, \tag{29}$$

therefore we can write,

$$u''(\omega t) + \{a - 2iq\sin(\omega t)\}u(\omega t) = 0, \tag{30}$$

$$v''(\omega t) + \{a + 2iq\sin(\omega t)\}v(\omega t) = 0. \tag{31}$$

Let us make the following change of variable $\phi' = \omega t/2$. By inserting this new variable in Equation (30), we obtain

$$u''(2\phi') + (A - 2iQ\sin 2\phi')u(2\phi') = 0 \tag{32}$$

where $A = 4a$ and $Q = 4q$. Notice that the equation for v (ωt) is obtained by the replacement of q by $-q$. Thus, we only need to solve Equation (32) for $q < 0$ and $q > 0$.

To find the spectrum of allowed energies, we follow a procedure similar to the one that we used for the case of intense electric fields. The main difference is that now Q is multiplied by the imaginary number i. In this case, we can still use the Floquet solution, and thus the spectrum is found by using Equations (21) and (22). However, $\Delta_r(0;\ a,\ q)$ is changed since the recursion relations are modified, as shown in Appendix 1.

Figure 2 shows the resulting energy spectrum. The gray zones are the allowed energy values, and again we obtain a series of bands. In the same plot we also present the contour curves corresponding to the same μ as given by Equation (21). This numerical result can be compared with a theoretical result by using perturbation theory, as shown in Appendix 2. In particular, in Appendix 2 we show that the separatrix between allowed and non-allowed states is given by,

$$A \approx \frac{1}{2}Q^2. \tag{33}$$

To compare the theoretical separatrix curve and the numerical transition curve at the origin, we calculated the curvature of the theoretical curve performing the second derivative of Equation (33). The theoretical result is 1 for the curvature, while the numerical result is 1.1.

The most important thing to notice in Figure 2 is that an energy gap appears near the Fermi energy ($\epsilon = 0$). As explained in Figure 3, where an amplification of the region around the origin is presented, for a given electric field, the minimal value of ϵ is determined by the separatrix curve. In fact, since the separatrix curve is given by $a \approx 2q^2$, and using Equations (28) and (29), we obtain the minimal allowed value of ϵ,

$$\epsilon \approx \pm\frac{\xi}{\sqrt{2}} \tag{34}$$

which produces a gap of size:

$$\Delta \approx \frac{\sqrt{2}ev_F E_0}{c\omega}. \tag{35}$$

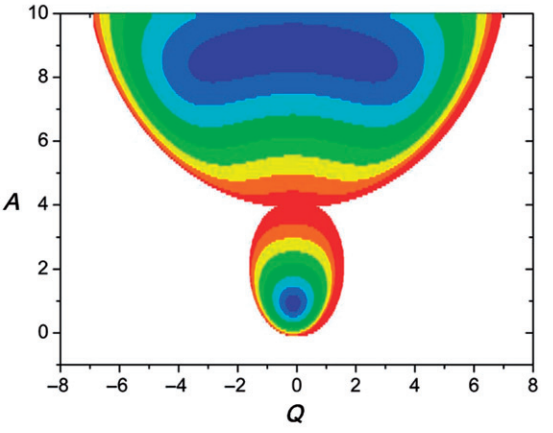

Figure 2. (Color online). Energy spectrum for the case of weak electric fields or short wavelengths. The gray zones are allowed energy values. Contours denote curves of the same μ.

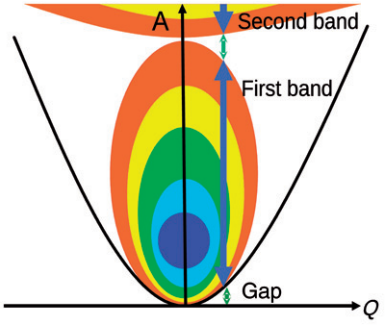

Figure 3. (Color online). Amplification of the energy spectrum for the case of weak electric fields around $\epsilon = 0$. For a fixed field (Q constant), the figure shows two energy gaps and two energy bands near the Fermi energy. The separatrix curve $A = Q^2/2$ obtained from perturbation theory (Appendix 2), which determines the minimal value of ϵ, is also shown.

Let us estimate this quantity, for a microwave frequency $\omega = 50$ GHz with an intensity $E_0 = 1$ V/m of the electric field, where the gap size is $\Delta \approx 0.03$ meV.

It is also worthwhile mentioning a second interesting prediction from Equation (33). One can observe that the spectrum is made mainly from stacked ellipses that grow in size, as seen in Figure 3. For $Q < 1.48$, the spectrum has two gaps, one around $A = 0$ and the other at $A = 4$. However, for $Q > 1.48$ both gaps merge and the first band disappears. Such a field is given by,

$$E_0 = \frac{1.48(c\hbar\omega^2)}{2ev_F},$$

for a typical microwave frequency $\omega = 50$ GHz. This value corresponds to a field of $E_0 = 1.797$ V/m.

4. Conclusions

In conclusion, we have found an equation that describes the interaction between charge carriers in graphene under electromagnetic radiation. By solving this equation we found the energy spectrum for intense electric fields and weak electric fields, as well as for short and long wavelengths. The main features of the spectra is that a gap is open near the Fermi energy. Thus, the conductivity can be controlled by applying an electromagnetic wave, which is an effect that could be useful to build electronic gates. Our analytical solution could also be useful to understand the optical properties of graphene.

Acknowledgements

We thank CONACyT 48783-F, 50368 and DGAPA-UNAM project IN 100310-3. Calculations were carried at the KanBalam Supercomputer of UNAM.

References

[1] A.K. Geim and K.S. Novoselov, Nature Mater. 6 (2007) p.183.
[2] A.H. Castro-Neto, Nature Mater. 6 (2007) p.179.
[3] A.H. Castro-Neto, F. Guinea, N.M.R. Peres, K.S. Novoselov and A.K. Geim, Rev. Mod. Phys. 81 (2009) p.109.
[4] K.S. Novoselov, A.K. Geim, S.V. Morozov, D. Jiang, Y. Zhang, S.V. Dubonos, I.V. Grigorieva and A.A. Firsov, Science 306 (2004) p.666.
[5] C. Lee, X. Wei, J.W. Kysar and J. Hone, Science 321 (2008) p.385.
[6] K.I. Bolotin, K.J. Sikes, Z. Jiang, M. Klima, G. Fudenberg, J. Hone, P. Kim and H.L. Stormer. Avalaible at http://arxiv.org/abs/0802.2389.
[7] J.H. Chen, C. Jang, S. Xiao, M. Ishigami and M. Fuhrer, Nature Nanotech. 3 (2008) p.206.
[8] L.A. Ponomarenko, F. Schedin, M.I. Katnelson, R. Yang, E.W. Hill, K.S. Novoselov and A.K. Geim, Science 320 (2008) p.356.
[9] Y.M. Lin, K.A. Jenkins, A. Valdes García, J.P. Small, D.B. Farmer and P. Avouris. Available at http://arxiv.org/abs/0812.1586v1.
[10] V.P. Gusynin and S.G. Sharapov, Phys. Rev. B 73 (2006) p.245411.
[11] V.P. Gusynin, S.G. Sharapov and J.P. Carbotte, Phys. Rev. Lett. 96 (2006) p.256802.
[12] S.A. Mikhailov and K. Ziegler, Phys. Rev. Lett. 99 (2007) p.016803.
[13] V. Lukose, R. Shankar and G. Baskaran, Phys. Rev. Lett. 98 (2007) p.116802.
[14] B. Trauzettel, Ya.M. Blanter and A.F. Morpurgo, Phys. Rev. B 75 (2007) p.035305.
[15] S. Krompiewski, Phys. Rev. B 80 (2009) p.075433.
[16] Y.M. Zuev, W. Chang and P. Kim, Phys. Rev. Lett. 102 (2009) p.096807.
[17] N.M.R. Peres, F. Guinea and A.H. Castro Neto, Phys. Rev. B 73 (2006) p.125411.
[18] L.A. Falkovsky and A.A. Varlamov. Available at http://arxiv.org/abs/cond-mat/0606800.
[19] S.A. Mikhailov, Europhys. Lett. 79 (2007) p.27002.
[20] F.J. López Rodríguez and G.G. Naumis, Phys. Rev. B. 78 (2008) p.201406.
[21] I. Synam, Phys. Rev. B 80 (2009) p.054303.
[22] G.G. Naumis, Phys. Rev. B 76 (2007) p.153403.
[23] A. Bostwick, J.L. McChesney, K. Emtsev, T. Seyller, K. Horn, S.D. Kevan and E. Rotenberg, Phys. Rev. Lett. 103 (2009) p.056404.
[24] D. Chandler. Available at www.physorg.com/news156698836.html.

[25] G.W. Semenoff, Phys. Rev. Lett. 53 (1984) p.2449.
[26] D.P. DiVicenzo and E.J. Mele, Phys. Rev. B 29 (1984) p.1685.
[27] J.C. Slonczewski and P.R. Weiss, Phys. Rev. 109 (1958) p.272.
[28] M. Lewkowicz and B. Rosenstein, Phys. Rev. Lett. 102 (2009) p.106802.
[29] J.A. Strang. Available at http://arxiv.org/PS_cache/math-ph/pdf/0510/0510076v2.pdf.
[30] E.T. Whittaker and G.N. Watson, *A Course Of Modern Analysis* , 4th ed., The Macmillan Company, New York, 1962.
[31] A.H. Nayfeh and D.T. Mook, *Nonlinear Oscillations*, John Wiley, New York, 1979.

Appendix 1

Here we provide the method used to find the energy spectrum of Equation (19). The energy spectrum for the complex case of q, given by Equation (32), can be found in a similar way.

If Equation (20) is inserted into Equation (19) the following recurrence relation is obtained,

$$C_{2r} + \frac{q}{(2r-\mu i)^2 - a}(C_{2r+2} + C_{2r-2}) = 0.$$

Defining

$$\gamma_{2r} = \frac{q}{(2r-\mu i)^2 - a}, \quad \vee r \in \mathbb{Z},$$

we obtain the following matrix,

$$\theta_r(\mu, a, q) = \begin{pmatrix} 1 & \gamma_{2r} & 0 & 0 & 0 & 0 & 0 \\ \gamma_{2r-2} & . & . & . & . & . & 0 \\ 0 & . & \gamma_0 & 1 & \gamma_0 & . & 0 \\ 0 & . & . & . & . & . & \gamma_{-2r+2} \\ 0 & 0 & 0 & 0 & 0 & \gamma_{-2r} & 1 \end{pmatrix}.$$

Finding non-trivial solutions of Equation (19) is equivalent to demanding,

$$\det(\theta_r(\mu; a, q)) = \Delta_r(\mu; a, q) = 0;$$

besides this give us the spectrum of energies. We are going to use a method proposed by Whittaker [30] for finding μ as a function of a and q.

Let us introduce the following quantity [30],

$$\lambda = \frac{1}{\cos(\pi i \mu) - \cos(\pi\sqrt{a})}.$$

This quantity has the same poles that $\det(\Delta_r(\mu;\, a,\, q)) = 0$ has. Besides,

$$\lim_{\mu \to \pm\infty} \lambda \sim \lim_{\mu \to \pm\infty} \frac{1}{e^{\pi\mu}} \to 0 \tag{36}$$

Therefore defining,

$$\eta = \Delta_r(\mu; a, q) - k\lambda, \tag{37}$$

we have that when $\mu \to \pm\infty$, η is bounded since,

$$\lim_{\mu \to \pm\infty} \eta = 1. \tag{38}$$

This result is a consequence of Equation (36) and the following fact,

$$\lim_{\mu\to\pm\infty}\Delta_r(\mu;a,q)=1. \tag{39}$$

Invoking Liouville's theorem due to the asymptotic behavior given by Equation (38), we have that

$$k=\frac{\Delta_r(\mu;a,q)-1}{\lambda} \tag{40}$$

must be a constant. Now we evaluate k for a particular $\Delta_r(\mu;a,q)$, for example at $\mu=0$. Thus

$$k=(\Delta_r(0;a,q)-1)(1-\cos\pi\sqrt{a}). \tag{41}$$

Using Equations (40) and (41) we obtain

$$\frac{\Delta_r(\mu;a,q)-1}{\lambda}=(\Delta_r(0;a,q)-1)(1-\cos\pi\sqrt{a}).$$

For our purposes $\Delta_r(\mu;a,q)=0$, and therefore

$$\mu=\frac{1}{\pi}\cos^{-1}(1-\Delta_r(0;a,q)(1-\cos\pi\sqrt{a}))\quad a\geq 0 \tag{42}$$

and

$$\mu=\frac{1}{\pi}\cos^{-1}(1-\Delta_r(0;a,q)(1-\cosh\pi\sqrt{a}))\quad a<0. \tag{43}$$

However, to plot the spectrum, the value of $\Delta_r(0;a,q)$ is missing. To evaluate this infinite determinant, we can use the recursive Strang method [29], which produces the following relation,

$$\Delta_r(0)=\beta_{2r}\Delta_{r-1}(0)-\alpha_{2r}\beta_{2r}\Delta_{r-2}(0)+\alpha_{2r}\alpha_{2r-2}^2\Delta_{r-3}(0),$$

where $\alpha_{2r}=\gamma_{2j}\gamma_{2j-2}$ and $\beta_{2r}=1-\alpha_{2r}$.

To solve the case of weak fields or short wavelengths, which is given by Equation (32), we need to consider that q is replaced by a complex iq in Equation (19). All the steps are similar to the real q case. However, the recurrence relation for $\Delta_r(0;a,q)$ is changed to,

$$\Delta_r(0)=\beta_{2r}\Delta_{r-1}(0)+\alpha_{2r}\beta_{2r}\Delta_{r-2}(0)-\alpha_{2r}\alpha_{2r-2}^2\Delta_{r-3}(0), \tag{44}$$

where $\alpha_{2r}=\gamma_{2j}\gamma_{2j-2}$ and $\beta_{2r}=1+\alpha_{2r}$.

Appendix 2

To find the separatrix between allowed and non-allowed states in Equation (30), we rewrite the equation as,

$$u''(2\phi')+(A-2iQsen2\phi')u(2\phi'))=0, \tag{45}$$

where we have made the change of variable $\omega t/2=\phi'$. Thus $A=4a$ and $Q=4q$. We seek solutions to Equation (45) in the form of the following perturbation expansions [31],

$$u(2\phi';Q)=u_0(2\phi')+Qu_1(2\phi')+Q^2u_2(2\phi')+\cdots \tag{46}$$

$$A=A_0+QA_1+Q^2A_2+\cdots. \tag{47}$$

Substituting Equations (46) and (47) into Equation (45) and equating coefficients of like powers of Q, we obtain,

$$u_0'' + A_0 u_0 = 0, \tag{48}$$

$$u_1'' + A_0 u_1 = -A_1 u_0 + 2iu_0 \sin 2\phi', \tag{49}$$

$$u_2'' + A_0 u_2 = -A_2 u_o - A_1 u_1 + 2iu_1 \sin 2\phi'. \tag{50}$$

Here we treat the case $A_0 = 0$. In this case $u_0 = \alpha$, α is a constant. Equation (49) becomes,

$$u_1'' = -A_1\alpha + 2i\alpha \sin 2\phi'. \tag{51}$$

In order to make u_1 periodic, we set $A_1 = 0$. Then the solution of Equation (51) is,

$$u_1 = -\frac{1}{2} i\alpha \sin 2\phi'. \tag{52}$$

Substituting u_0 and u_1 into Equation (50) yields,

$$u_2'' = -A_2\alpha + \alpha \sin^2 2\phi', \tag{53}$$

thus,

$$u_2'' = -A_2\alpha + \frac{\alpha}{2}(1 - \cos 4\phi'). \tag{54}$$

To ensure that u_2 is periodic, we let $A_2 = \frac{1}{2}$. Hence the separatrix curve emanating from the origin is given by

$$A = \frac{1}{2} Q^2 + O(Q^3), \tag{55}$$

and the wave function obtained after solving Equation (54) is

$$u = \alpha\left(1 - \frac{iQ}{2} \sin 2\phi' + \frac{Q^2}{32} \cos 4\phi' + \cdots\right). \tag{56}$$